

Lecture note Magnetism (10)

15th June (2022) Shingo Katsumoto, Institute for Solid State Physics, University of Tokyo

Last week, we have seen the Holstein-Primakoff transformation. However, we have skipped some elementary explanation on the classical view of the spin wave, and here I added some explanations in Appendix 10A.

Why we need to introduce the method of Holstein-Primakoff transformation? Because the variable in the Hamiltonian is now spin, which differs from the canonical variables in classical mechanics such as a spatial coordinate of an electron, and the ordinary general method of quantum field theory cannot be applied. Various problems in the Holstein-Primakoff way were pointed out, e.g., in [1]. A particularly problematic is the “extension” of functional space for n over $2S$ in the form of eq. (5.72). It is proven that the operators of physical quantities have no matrix element between the original functional space and the extended space[2]. However we need to be careful that the proof is for exact theories and some approximations may create some elements. We can escape the problem in treating small n cases.

In the quantization of the Heisenberg model by the Holstein-Primakoff method, the quantized bosons have mutual interaction due to the non-linear term in eq. (5.73). In order to ignore the interaction and to treat it as the sum of harmonic oscillators, we apply the following approximation. The expansions of eq. (5.73) with \hat{n} :

$$\left. \begin{aligned} \hat{S}_{j+} &= \sqrt{2S} \left(1 - \frac{a_j^\dagger a_j}{4S} + \dots \right) a_j, \\ \hat{S}_{j-} &= \sqrt{2S} a_j^\dagger \left(1 - \frac{a_j^\dagger a_j}{4S} + \dots \right), \end{aligned} \right\} \quad (5.74)$$

are substituted to the Heisenberg model, to get

$$\begin{aligned} \mathcal{H} &= -2 \sum_{\langle i,j \rangle} J_{ij} \hat{S}_i \cdot \hat{S}_j = -2 \sum_{\langle i,j \rangle} J_{ij} \{ \hat{S}_{iz} \hat{S}_{jz} + (\hat{S}_{i+} \hat{S}_{j-} + \hat{S}_{i-} \hat{S}_{j+})/2 \} \\ &= -2 \sum_{\langle i,j \rangle} J_{ij} \left[S^2 - S(\hat{n}_i + \hat{n}_j) + S(a_i^\dagger a_j + a_j^\dagger a_i) + \hat{n}_i \hat{n}_j - \frac{1}{4} a_i^\dagger a_j^\dagger a_j a_i - \frac{1}{4} a_j^\dagger a_i^\dagger a_i a_j + \dots \right], \end{aligned} \quad (5.75)$$

where $\hat{n}_i = a_i^\dagger a_i$. We take the terms to quadratic of a_i, a_i^\dagger to reach

$$\mathcal{H} = -2 \sum_{\langle i,j \rangle} J_{ij} [S^2 - S(\hat{n}_i + \hat{n}_j) + S(a_i^\dagger a_j + a_j^\dagger a_i)]. \quad (5.76)$$

The result is the same if we take the terms with S in them.

We define the Fourier transform of a_j^\dagger, a_j as

$$\left. \begin{aligned} a_{\mathbf{q}} &= \frac{1}{\sqrt{N}} \sum_j a_j \exp(i\mathbf{q} \cdot \mathbf{r}), \\ a_{\mathbf{q}}^\dagger &= \frac{1}{\sqrt{N}} \sum_j a_j^\dagger \exp(-i\mathbf{q} \cdot \mathbf{r}). \end{aligned} \right\} \quad (5.77)$$

With substituting the above, the Hamiltonian is finally given by

$$\begin{aligned} \mathcal{H} &= -2 \sum_{\langle i,j \rangle} J_{ij} S^2 + 2 \sum_{\mathbf{q}} [J_0 - J_{\mathbf{q}}] S a_{\mathbf{q}}^\dagger a_{\mathbf{q}} \\ &= E_0 + \sum_{\mathbf{q}} \hbar \omega_{\mathbf{q}} a_{\mathbf{q}}^\dagger a_{\mathbf{q}}, \end{aligned} \quad (5.78)$$

which is in the form of a set of spin waves without mutual interaction. In this way, we can take into account the interaction systematically with taking the higher order terms one by one. Such quantized spin waves as bosons are called **magnons**.

5.8.3 Magnon approximation of low energy excitations

As we saw in the derivation of eq. (5.76), the approximation of harmonic oscillators corresponds to the ignorance of the interaction between magnons. The approximation is not good for many-magnon excitation at high temperatures. We thus consider the contributions of magnons to physical quantities at low temperatures. With taking the magnetic field along z -axis, the magnetization is

$$M = \mu \left\langle \sum_i S_{iz} \right\rangle = \mu SN - \mu \sum_i \langle a_i^\dagger a_i \rangle = \mu SN - \mu \sum_{\mathbf{q}} n(\epsilon_{\mathbf{q}}), \quad (5.79)$$

where

$$n(\epsilon) = \left(\exp \frac{\epsilon}{k_B T} - 1 \right)^{-1} \quad (5.80)$$

is the Bose distribution function. From eq. (5.78), $\hbar\epsilon_{\mathbf{q}} = 2S(J_0 - J_{\mathbf{q}})$. We assume the exchange interaction J works only between nearest neighbors. We here consider a square lattice. Let a be the distance of nearest neighbors and q vector be along a lattice direction. Then

$$\hbar\epsilon_{\mathbf{q}} = 2S(J_0 - J_{\mathbf{q}}) = 2SJ\{2 - [\exp(iqa) + \exp(-iqa)]\} \simeq 2SJ \left[2 - 2 \left(1 - \frac{(qa)^2}{2} \right) \right] = 2SJ(qa)^2. \quad (5.81)$$

From the above, with use of the low temperature asymptotic form of the Bose distribution function, M is given by

$$M = \mu N \left[S - \zeta \left(\frac{3}{2} \right) \left(\frac{k_B T}{8\pi JS} \right)^{3/2} \right], \quad (5.82)$$

where $\zeta(x)$ is the Riemann's ζ -function and $\zeta(3/2) \approx 2.61$.

Next, we consider the specific heat at low temperatures. The internal energy is obtained from the low temperature asymptotic form of the Bose function and the dispersion relation as

$$U = E_0 + \sum_{\mathbf{q}} n(\epsilon_{\mathbf{q}}) \hbar\epsilon_{\mathbf{q}} = E_0 + 12\pi JSN \zeta \left(\frac{5}{2} \right) \left(\frac{k_B T}{8\pi JS} \right)^{5/2}, \quad (5.83)$$

from which the specific heat is obtained as

$$C = \frac{\partial U}{\partial T} = \frac{15}{4} N k_B \zeta \left(\frac{5}{2} \right) \left(\frac{k_B T}{8\pi JS} \right)^{3/2}. \quad (5.84)$$

5.8.4 Anti-ferromagnetic spin wave

Next we proceed to the anti-ferromagnet. As in Sec. 5.5, we consider A and B sublattices with antiparallel magnetizations. We assume ferromagnetic Holstein-Primakoff transform can be applied to A-sublattice. Then a magnon propagation in A-sublattice affects spins in B-sublattice and causes propagation of precession around z -axis. However in B-sublattice the direction of the effective field is inverse and the direction of precession should be inverse. Consequently, the system can be described as coexistence of two-types of magnons with a mutual interaction. Then we need to consider another kind of bosons in B-sublattice. The vacuum should be the inverse of that in A-sublattice and $|0\rangle_B = |-S\rangle$. Then for site j in B-sublattice $j (j \in B)$, we introduce the transform

$$\left. \begin{aligned} S_{jz} &= -S + b_j^\dagger b_j, \\ S_{j+} &= b_j^\dagger \sqrt{2S - b_j^\dagger b_j}, \\ S_{j-} &= \sqrt{2S - b_j^\dagger b_j} b_j. \end{aligned} \right\} \quad (5.85)$$

As in the case of ferromagnet, (5.73) and (5.85) are substituted into the anti-ferromagnetic Heisenberg model. Then taking to quadratic of boson operators,

$$\mathcal{H} = -\alpha_z |J| N S^2 + 2|J| S \sum_{\langle i,j \rangle} (a_i^\dagger a_i + b_j^\dagger b_j + a_i b_j + a_i^\dagger b_j^\dagger), \quad (5.86)$$

where $i \in A, j \in B$. Let the Fourier transform of a_i, b_j be written as

$$\left. \begin{aligned} a_i &= \sqrt{\frac{2}{N}} \sum_{\mathbf{q}} a_{\mathbf{q}} \exp(-i\mathbf{q} \cdot \mathbf{r}_i), \\ b_j &= \sqrt{\frac{2}{N}} \sum_{\mathbf{q}} b_{\mathbf{q}} \exp(-i\mathbf{q} \cdot \mathbf{r}_j), \end{aligned} \right\} \quad (5.87)$$

then the Hamiltonian is re-written as

$$\mathcal{H} = -\alpha_z |J| N S^2 + 2\alpha_z |J| S \sum_{\mathbf{q}} [a_{\mathbf{q}}^\dagger a_{\mathbf{q}} + b_{\mathbf{q}}^\dagger b_{\mathbf{q}} + \gamma(\mathbf{q})(a_{\mathbf{q}}^\dagger b_{\mathbf{q}}^\dagger + a_{\mathbf{q}} b_{\mathbf{q}})], \quad (5.88)$$

where $\gamma(\mathbf{q})$ is defined as

$$\gamma(\mathbf{q}) = \alpha_z^{-1} \sum_{\boldsymbol{\rho}} \exp(-i\mathbf{q} \cdot \boldsymbol{\rho}) \quad (5.89)$$

with $\boldsymbol{\rho}$ a vector connecting interacting two spins.

For the diagonalization of the Hamiltonian, we introduce the **Bogoliubov transformation** $(a_{\mathbf{q}}, b_{\mathbf{q}}) \rightarrow (\alpha_{\mathbf{q}}, \beta_{\mathbf{q}})$ as

$$\left. \begin{aligned} a_{\mathbf{q}} &= \cosh \theta_{\mathbf{q}} \alpha_{\mathbf{q}} - \sinh \theta_{\mathbf{q}} \beta_{\mathbf{q}}^\dagger, \\ b_{\mathbf{q}} &= \cosh \theta_{\mathbf{q}} \beta_{\mathbf{q}} - \sinh \theta_{\mathbf{q}} \alpha_{\mathbf{q}}^\dagger. \end{aligned} \right\} \quad (5.90)$$

$(\alpha_{\mathbf{q}}, \beta_{\mathbf{q}})$ satisfy the following boson commutation relations,

$$[\alpha_{\mathbf{q}}, \alpha_{\mathbf{q}}^\dagger] = 1, \quad [\beta_{\mathbf{q}}, \beta_{\mathbf{q}}^\dagger] = 1, \quad [\alpha_{\mathbf{q}}, \beta_{\mathbf{q}}] = [\alpha_{\mathbf{q}}^\dagger, \beta_{\mathbf{q}}^\dagger] = 0. \quad (5.91)$$

The Hamiltonian reads

$$\begin{aligned} \mathcal{H} = -\alpha_z |J| N S^2 + 2\alpha_z |J| S \sum_{\mathbf{q}} [(\cosh 2\theta_{\mathbf{q}} - \gamma(\mathbf{q}) \sinh \theta_{\mathbf{q}})(\alpha_{\mathbf{q}}^\dagger \alpha_{\mathbf{q}} + \beta_{\mathbf{q}}^\dagger \beta_{\mathbf{q}} + 1) \\ - 1 - (\sinh 2\theta_{\mathbf{q}} - \gamma(\mathbf{q}) \cosh 2\theta_{\mathbf{q}})(\alpha_{\mathbf{q}} \beta_{\mathbf{q}} + \alpha_{\mathbf{q}}^\dagger \beta_{\mathbf{q}}^\dagger)]. \end{aligned} \quad (5.92)$$

For the last off-diagonal term to vanish, we should choose the parameter $\theta_{\mathbf{q}}$ as

$$\sinh 2\theta_{\mathbf{q}} / \cosh 2\theta_{\mathbf{q}} = \tanh 2\theta_{\mathbf{q}} = \gamma(\mathbf{q}). \quad (5.93)$$

Hence the diagonalized Hamiltonian is given by

$$\mathcal{H} = -\alpha_z |J| N S^2 + 2\alpha_z |J| S \sum_{\mathbf{q}} [(\sqrt{1 - \gamma(\mathbf{q})^2} - 1) + \sqrt{1 - \gamma(\mathbf{q})^2}(\alpha_{\mathbf{q}}^\dagger \alpha_{\mathbf{q}} + \beta_{\mathbf{q}}^\dagger \beta_{\mathbf{q}})]. \quad (5.94)$$

In eq. (5.94), the first two terms without operator represent the ground state energy. The first term is the energy of Néel ordered state. The second term can be interpreted as the zero-point motion energy of magnons. The classical Néel ordered state is not the quantum mechanical ground state unlike the ferromagnetic case. Namely the original $S_{jz} = S, S-1, \dots, -S$ states are hybridized though the anti-ferromagnetic interaction and the perturbation decreases the ground state energy. Accordingly, the expectation value of spin size diminishes from the full-size of S . The amount of the decrease is

$$\langle S_{jz} \rangle = S - \frac{2}{N} \sum_{\mathbf{q}} \sinh \theta_{\mathbf{q}} = S - \frac{1}{N} \sum_{\mathbf{q}} \left(\frac{1}{\sqrt{1 - \gamma(\mathbf{q})^2}} - 1 \right). \quad (5.95)$$

The table below shows the decreases in spin size ($\Delta = S - \langle S_{jz} \rangle$), and the variation in energy (ϵ is defined as $E_0 = N|J|\alpha_z S(S + \epsilon)$), calculated for some simple lattice structures[3].

Lattice	Square	Simple Cubic	Body Centered Cubic
Δ	0.917	0.078	0.0593
ϵ	$0.158+0.0062S^{-1}$	$0.097+0.0024S^{-1}$	$0.073+0.0013S^{-1}$

The anti-ferromagnetic magnons expressed by the last two terms, degenerate reflecting the equivalency of A- and B-sublattices. The dispersion relation is obtained from

$$\epsilon_{\mathbf{q}} = 2\alpha_z |J| S \sqrt{1 - \gamma(\mathbf{q})^2}. \quad (5.96)$$

$\gamma(\mathbf{q})$ defined in eq. (5.89) can be calculated, e. g., for simple cubic lattice with a unit cell size a , the dispersion in the long wavelength limit is given by

$$\epsilon_{\mathbf{q}} = 2\sqrt{2\alpha_z} |J| S a q, \quad (5.97)$$

which is linear in q .

Specific heat is a quantity to be compared with experiments. As in the case of ferromagnet, we consider the internal energy which is given in the case of simple cubic lattice by

$$U = E_0 + \frac{\pi^2}{15} N \left(\frac{k_B T}{2\sqrt{2\alpha_z} |J| S} \right)^3 k_B T, \quad (5.98)$$

where E_0 is the ground state energy given by the first two terms in eq. (5.94). The calculated specific heats are summarized in the following table including the cases of 1D, 2D, etc.[3].

Lattice	1D Chain	2D Square Lattice	3D Simple Cubic
$\frac{E_0}{\alpha_z J N S^2}$	$1+0.363S^{-1}$	$1+0.158S^{-1}$	$1+0.097S^{-1}$
$\frac{C}{N k_B}$	$\frac{2\pi}{3} \left(\frac{k_B T}{2\alpha_z J S} \right)$	$\frac{14.42}{\pi} \left(\frac{k_B T}{2\alpha_z J S} \right)^2$	$4\sqrt{3} \frac{\pi^2}{5} \left(\frac{k_B T}{2\alpha_z J S} \right)^3$
ΔS	Diverge	0.197	0.078

The original purpose of considering magnons is to treat thermal fluctuation at low temperatures correctly. Particularly for anti-ferromagnets, there are real materials close to the theoretical models. Hence it is important whether the simple models can explain such experiments. Figure 5.8 shows the crystal structure and the measured specific heat of an organic

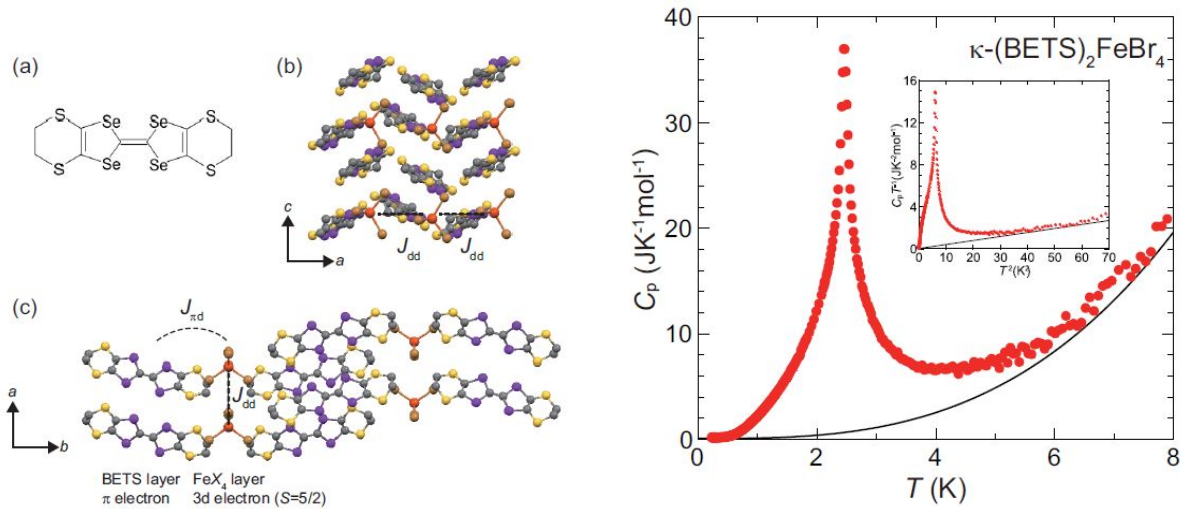


Fig. 5.8 Crystal structure and specific heat of κ -(BETS) $_2$ FeX $_4$. Left: (a) Molecular structure of BETS. (b) Crystal structure viewed from b -axis. BETS molecules are in line with alternative oblique angles. (c) Crystal structure viewed from c -axis. Right: Low temperature specific heat of a sample with X=Br. The contribution from phonons with T^3 dependence is indicated by a black line. The inset shows $C_p T^{-1}$ as a function of T^2 [4].

anti-ferromagnet κ -(BETS)₂FeBr₄ (BETS = bis(ethylenedithio)tetraselenafulvalene)[4]. This material is not an insulator having metallic conductivity. At low temperatures, it undergoes an anti-ferromagnetic transition at $T_N = 2.47$ K, and further, a superconducting transition at 1.1 K. The crystal shown in the left panel is composed of stacking of comparatively small molecules. Electrons in π -bonds spread over ab plane, which is stacked along c -axis. The anti-ferromagnetism originates from $3d$ -electrons in Fe with $S = 5/2$. There are J_{dd} , which is direct interaction between d 's, and $J_{\pi d}$, which is mediated by π .

The right panel in Fig. 5.8 displays the measured specific heat, which shows very sharp increase at T_N . This corresponds to the jump at T_C in the figure in Sec. 5.3. The inset shows C_p/T as a function of T^2 . An ordinary metal has a specific heat $C_m = AT + BT^3$ from an electron contribution ($\propto T$) and a lattice contribution ($\propto T^3$). This is written as $C_m/T = A + BT^2$ and expressed as a line in this plot. The contribution of electrons is negligibly small as known from the fitting at high temperatures. The heat capacity shows T^2 -like variation in the region lower than T_N , as it shows a line. This seems to be in accordance with the result of 2D specific heat in the above table. In the paper, however, the authors claim that the results are in accordance with a theory on 1D anti-ferromagnetic chain.

5.8.5 Nambu-Goldstone theorem and spin wave

In the section of ferromagnetic transition in Heisenberg model, we have visited the concept of spontaneous symmetry breaking (SSB). In typical continuous phase transitions, a symmetry should be spontaneously broken and at the same time an order appears.

Nambu-Goldstone theorem is summarized as follows:

Nambu-Goldstone theorem

When a symmetry of a physical system is spontaneously broken, there is an excitation with zero energy (gap) in the long wavelength limit.

Sometimes it is described as “excitation with zero-mass.” From the still energy $E = mc^2$, the two descriptions are equivalent.

This can be intuitively understood in the case of ferromagnetic transition. In the phenomenology in Sec. 5.2, as (a)→(b) in Fig. 5.2, the SSB caused by appearance of two minima in the free energy $\mathcal{F}(M)$. For example, two-dimensional Heisenberg model is isotropic and in the SSB state, the free energy of the state $(M_0 \cos \theta, M_0 \sin \theta)$ does not depend on θ , in other words, the state can freely go around on the yellow line in the figure. The motion on the yellow line is **Nambu-Goldstone mode** (NG mode) in the present case. This corresponds to the rotation of macroscopic magnetization

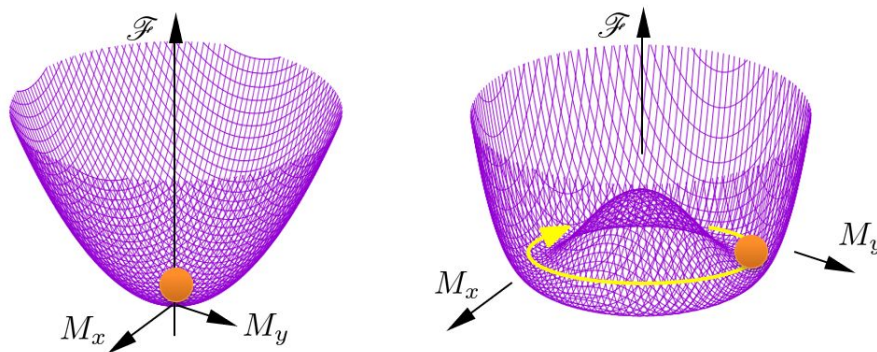


Fig. 5.9 Left: Free energy \mathcal{F} of a system with rotational symmetry. The lowest \mathcal{F} is obtained at M (magnetization)=0 on (M_x, M_y) plane. Right: A spontaneous symmetry breaking yields an order parameter (magnetization). The states with minimum \mathcal{F} exist continuously, between which the system can transit without energy (Nambu-Goldstone mode).

and can be seen as the limit of long wavelength. Classically the magnon wavelength is determined by the phase shift of precessions between neighboring sites. In the long wavelength limit, the phase shift is zero, and the spins are rotating coherently. Hence we can say the magnon is the NG mode in the present case.

The dispersion relation of ferromagnetic magnon is quadratic in q as eq. (5.81). On the other hand in the anti-ferromagnetic magnons, the dispersion is linear as in eq. (5.96). Sometimes the latter is called type-A and the former is called type-B NG mode. On the other hand Nielsen-Chadha[5] called $\hbar\omega \propto k^{2n+1}$ as type-I, $\hbar\omega \propto k^{2n}$ as type-II.

As is well known, it originated from Yoichiro Nambu's idea for the acquisition of particle mass on the superconducting BCS theory as a model, and from there, the standard theory of elementary particles makes great progress. And also in the condensed matter theory, it is one of the central concepts as introduced by Anderson in the book "basic notions"[6]. Even though there are many open questions even in the basics of the NG mode. Surprisingly there are many important findings and progresses recently. Here I introduce an example. In the naïve NG theorem, the number of broken symmetries N_{BS} and that of NG modes N_{NG} should be the same ($N_{BS} = N_{NG}$). However that does not hold in many simple examples. In the case of 3D ferromagnetic transition, the rotation symmetries of two axes are broken, hence $N_{BS} = 2$ though simple ferromagnetic magnon NG mode number is one, i.e., $N_{NG} = 1$.

For this problem, based on the pioneering works by Nielsen-Chadha[5] and by others, Watanabe-Murayama[7], and Hidaka[8] reached the satisfactory answer in 2012 independently. This can be viewed as a generalization of the NG theorem. To say it very short, let N_I and N_{II} be the number of type-I and type-II NG modes respectively, then

$$N_I + 2N_{II} = N_{BS}.$$

For the detail see the review paper[9].

5.9 Experiments on magnons

As we saw in the above, magnons are elementary excitations from the ground state, considered to calculate macroscopic quantities of magnetic materials at finite temperatures. However recently, the concept of magnon goes beyond the framework. The researches are prosperous on the wave and the particle like manners, soliton physics or Bose-Einstein condensation in the high-density non-linear region where the original spin wave approximation does not hold. The birth is given to the word "magnonics" and application to quantum information processing is seriously considered[10]. You can find many reviews[11] and textbooks[12].

Here I would like to introduce rather old results, which are now the basis of present studies, however.

5.9.1 Measurement of magnon dispersion relation by neutron scattering

Neutron scattering has long been used as a means of measuring microscopic magnetic structures. It can be said that it is still the most powerful reliable experimental method with atomic resolution. Inelastic scattering was used, in particular, for magnon dispersion measurements.

We write the interaction between the magnetic moment μ_e of electrons in an atom and that of a neutron as

$$\mathcal{H}_{\text{int}} = -\mu_e \cdot \mathbf{B}_n, \quad (5.99)$$

where

$$\mathbf{B}_n = \text{rot} \left(\mu_n \times \frac{\mathbf{r}}{r^3} \right) \quad (5.100)$$

is the magnetic field of neutron magnetic moment μ_n , \mathbf{r} is the vector connecting the atom and the neutron. When a neutron is scattered by such an interaction as

$$\hbar\mathbf{k} \longrightarrow \hbar(\mathbf{k} - \mathbf{q}), \quad (5.101)$$

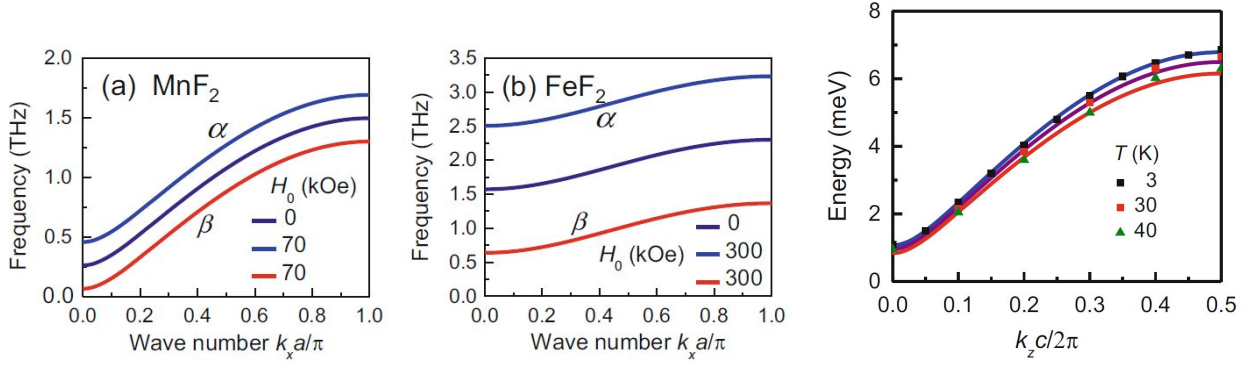


Fig. 5.10 (a), (b) Magnon dispersion relations calculated for MnF₂, FeF₂ incorporating anisotropic field[12]. Right panel: Magnon dispersion relation measured in MnF₂ by time of flight method of neutron scattering[13].

the variation in the energy is

$$\Delta E = \frac{\hbar^2}{2M}(-2\mathbf{k} \cdot \mathbf{q} + \mathbf{q}^2). \quad (5.102)$$

In very short, pulses of neutron with appropriate energy is applied to the sample, and the measurements of the energy (momentum) change and the scattering angle give certain information. This is (in the case of $\Delta E \neq 0$) the **inelastic scattering** of neutron. On the other hand in the case of elastic scattering ($\Delta E = 0$), the wave nature of neutrons the diffraction is important.

To obtain the dispersion relation of magnons, the inelastic scattering of neutron is mostly used. Figure 5.10 shows the magnon dispersion relation of MnF₂ obtained by neutron inelastic scattering. For the above information of (5.101) and (5.102), time-of-flight (TOF) method was utilized[13]. The result shows a good agreement with the result of molecular field approximation with the effect of anisotropy.

5.9.2 Bose-Einstein condensation of magnons

In the process of introducing magnons with creation/annihilation operators, we defined the vacuum $|0\rangle_F$ as $|S\rangle$, i.e., the state of $S_z = S$, and $|n\rangle_F$ as $|S - n\rangle$. As mentioned, while we do not have negative n state from the definition, repetitive operation of creation operator creates infinite number of n states. However in reality, S_z can take only down to $-S$. This physical space of function does not have any matrix element with the extended space as long as the theory is exact (no approximation). This means that the magnons, though their creation/annihilation operators satisfy bosonic commutation relations, the condition that “a single state can accommodate an infinite number of particles” is not fulfilled. In this sense, the statistics of magnon is not complete Bose statistics but a para-statistics[14].

A typical phenomenon appeared in the system of bosons is the **Bose-Einstein Condensation** (BEC). The BEC is very shortly introduced in Appendix 10B. Superfluidity of helium, BEC in laser-cooled neutral atomic gases are the representatives. Even for these phenomena, the interaction between the particles exists and they are not just the same as the simple BEC described in the Appendix. Also, the superconductivity, in which weakly bound fermion pairs condensate is a similar phenomenon. Even in the case of magnons, though they obey para-statistics, they can be viewed as “bosons with hard cores” and there is a possibility that a similar phenomenon occurs. It is still difficult, though, for magnons to fulfill the basic condition of BEC that (averaged de Broglie wavelength)=(averaged particle distance) because the particle density decreases with lowering the temperature, as is guessed from the calculation of the magnetization in eq. (5.79). Then an experiment was carried out, in which a large number of magnons are excited by microwave and a non-equilibrium BEC took place[15]. They studied the Brillouin scattering of light by magnons and observed anomalous narrowing of the linewidth of the resonance.

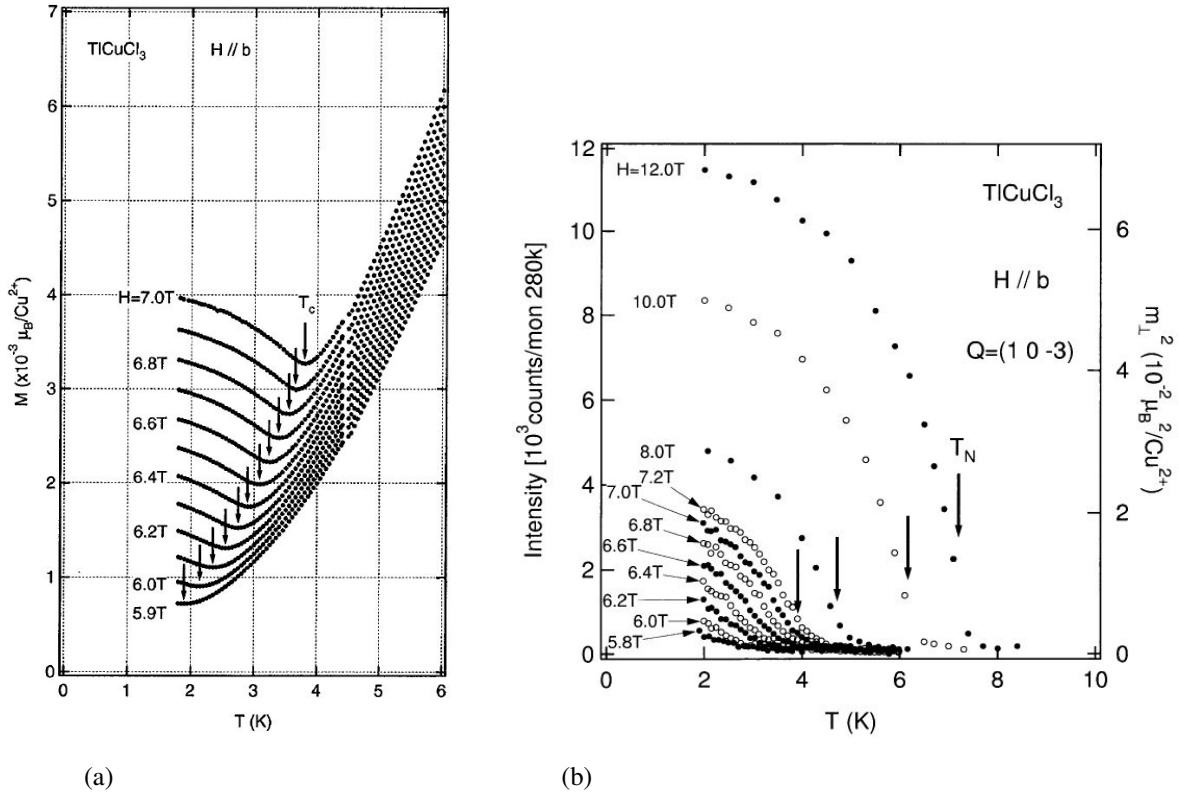


Fig. 5.11 (a) Temperature dependent magnetization of TiCuCl_3 in magnetic fields[16], (b) Temperature variation of the intensity of Bragg reflection $(1,0,-3)$ in neutron diffraction[17]. As indicated in the right axis, this is proportional to the square of vertical magnetic moment per site.

Let us see an experimental observation of BEC in thermal equilibrium[16, 17]. Due to the above restriction, the situation is rather special. The material is a compound of TiCuCl_3 in chemical formula. Two magnetic ions form pairs (dimer) with an antiferromagnetic coupling. There are singlet $|0,0\rangle$ and triplet $(|1,-1\rangle, |1,0\rangle, |1,1\rangle)$ as the states of the pair, in which the single is the ground state due to the antiferromagnetic coupling. There is an energy gap (spin gap) between the ground state and the first excited state. With applying magnetic field, the energy of $|1,1\rangle$ is lowered and the field driven phase transition takes place for the ferromagnetism to appear. In this system, the magnon appears when the energies of $|0,0\rangle$ and $|1,1\rangle$ are close as the propagation of $|1,1\rangle$ states to the neighboring sites. As known from this example, the propagation of magnons is the equivalent to that of spin angular momentum and that brings a **spin current**. For the behavior of magnetization in such a system without magnon BEC, a theory has been presented [18] and the high temperature behavior is well explained. It predicts for the the magnetization transverse to the spontaneous magnetization that it should be constant for temperature. However in the experiment, as in Fig. 5.11(a) the magnetization once decreases with decrease of temperature but the dependence is inverted around the transition point and increases. The magnon-BEC theory explains the experiment that an order grows in the mixture of $|0,0\rangle$ and $|1,1\rangle$ and the transverse magnetization appears as an average (does not cancel out)[16]. Furthermore as in Fig. 5.11(b) in neutron diffraction, it was confirmed that such an order actually grows[17]. From the above, the observation of magnon BEC is claimed.

Appendix 10A: Collective motion of spins

Because a macroscopic number of spins are bound to in a ferromagnetic state, the motion can be described as a collective motion. On the other hand, as lattice vibrations in lattice formation, a kind of collective motion from the magnetic ground state can exist and quantization as phonons is possible.

10A.1 Collective motion of magnetization

For a ferromagnetic total magnetization

$$\mathbf{S} = \sum_i \mathbf{S}_i, \quad (10A.1)$$

we apply Heisenberg equation of motion as

$$i\hbar \frac{\partial \mathbf{S}}{\partial t} = [\mathbf{S}, \mathcal{H}], \quad (10A.2)$$

which is formally the same as eq. (2.11) and represents the Larmor precession. A resonance experiment as EPR for a total magnetization is possible and called as **ferromagnetic resonance** (FMR). From FMR we get various information on the ferromagnetism and the spin wave.

Next we consider the case that the phase of the precession has a constant shift between neighboring spins. The above motion of the total magnetization can be considered as the long wavelength limit of this motion. The magnetization and the external field direction is taken to z . This situation is expressed as

$$S_{ix} = A \cos(\omega_0 t + \theta_i), \quad S_{iy} = A \sin(\omega_0 t + \theta_i), \quad (10A.3)$$

with a shift of θ_i with i . Let us use complex numbers for spins. And the Fourier transform and the inverse transform

$$S_{qx} = \frac{1}{\sqrt{N}} \sum_j S_{jz} \exp(-i\mathbf{q} \cdot \mathbf{r}_j), \quad S_{jx} = \frac{1}{\sqrt{N}} \sum_q S_{qx} \exp(i\mathbf{q} \cdot \mathbf{r}_j) \quad (10A.4)$$

are introduced.

We apply (10A.2) to Heisenberg Hamiltonian $\mathcal{H} = -2J \sum_{\langle i,j \rangle} \hat{\mathbf{S}}_i \cdot \hat{\mathbf{S}}_j$ to obtain the following.

$$i\hbar \frac{\partial S_{qx}}{\partial t} = \frac{4i}{\sqrt{N}} J \sum_{\langle i,j \rangle} S_{iy} S_{jz} \exp(-i\mathbf{q} \cdot \mathbf{r}_i) \{1 - \exp[i\mathbf{q} \cdot (\mathbf{r}_i - \mathbf{r}_j)]\} \quad (10A.5a)$$

$$i\hbar \frac{\partial S_{qy}}{\partial t} = -\frac{4i}{\sqrt{N}} J \sum_{\langle i,j \rangle} S_{ix} S_{jz} \exp(-i\mathbf{q} \cdot \mathbf{r}_i) \{1 - \exp[i\mathbf{q} \cdot (\mathbf{r}_i - \mathbf{r}_j)]\}. \quad (10A.5b)$$

Fourier transform of J is written as

$$J_q = \sum_j J \exp[i\mathbf{q} \cdot (\mathbf{r}_i - \mathbf{r}_j)]. \quad (10A.6)$$

In the above, the sum over j and i can be taken anywhere because the interaction only depends on $\mathbf{r}_i - \mathbf{r}_j$. Further, the sum only over the nearest neighbor because the interaction is assumed to work only for nearest neighbors. Here we approximate S_{jz} by S , which corresponds to small angle approximation. Then

$$\hbar \frac{\partial S_{qx}}{\partial t} = 2[J_0 - J_q] S S_{qy}, \quad (10A.7a)$$

$$\hbar \frac{\partial S_{qy}}{\partial t} = -2[J_0 - J_q] S S_{qx}. \quad (10A.7b)$$

This is the same as eq. (5.68) but with $B = 0$.

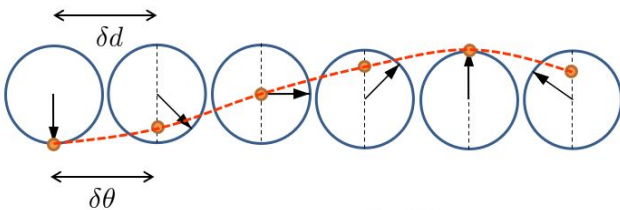


Fig. 10A.1 Schematic diagram showing a constant phase shift between neighboring spins.

Appendix 10B: Bose-Einstein condensation

The Bose-Einstein Condensation (BEC)^{*1} is called a phase transition that is not due to the interaction between freedoms (quantum statistical phase transition). Though phase transitions caused by interaction between some freedoms can be intuitively understood, there are different types of phase transitions, in which the transitions are caused as the results of competition between various factors. A representative is BEC.

In the case of bosonic systems, in spite of the absence of “force” between the particles, there exists the tendency for them to occupy the same quantum state originating from their statistical property. Let us see that for the case of two particles. We write a solution of the wave equation for two particles as $\psi(\mathbf{x}_1, \mathbf{x}_2)$. For the composition of wavefunctions of the system $\Psi(\mathbf{x}_1, \mathbf{x}_2)$ that reflects the statistical property of bosons, the symmetrization of ψ results in

$$\Psi(\mathbf{x}_1, \mathbf{x}_2) = \frac{1}{\sqrt{2}} [\psi(\mathbf{x}_1, \mathbf{x}_2) + \psi(\mathbf{x}_2, \mathbf{x}_1)]. \quad (10B.1)$$

Hence the probability of finding the system at $(\mathbf{x}_1, \mathbf{x}_2)$ is

$$|\Psi(\mathbf{x}_1, \mathbf{x}_2)|^2 = \frac{1}{2} [|\psi(\mathbf{x}_1, \mathbf{x}_2)|^2 + |\psi(\mathbf{x}_2, \mathbf{x}_1)|^2 + \psi(\mathbf{x}_1, \mathbf{x}_2)^* \psi(\mathbf{x}_2, \mathbf{x}_1) + \psi(\mathbf{x}_1, \mathbf{x}_2) \psi(\mathbf{x}_2, \mathbf{x}_1)^*]. \quad (10B.2)$$

This reveals that the last two interference terms intensify the probability of finding the system under the condition of $\mathbf{x}_1 = \mathbf{x}_2$. Let us write the de Broglie wavelength as λ and the averaged distance between the particles as l . Then at low temperatures $\lambda \sim l$, this tendency of bosons makes many of them to occupy the state of $k = 0$, which behavior leads to BEC. The above discussion is expressed as

$$\begin{aligned} E_k &= \frac{p^2}{2M} = k_B T, \\ \Delta p &\sim \sqrt{M k_B T} \\ \therefore \lambda &= \frac{h}{\Delta p} \sim \frac{h}{\sqrt{M k_B T}}. \end{aligned} \quad (10B.3)$$

λ elongates as $1/\sqrt{T}$ with lowering the temperature. And with growing of the overlapp between the single particle wavefunctions makes them undistinguishable and the symmetrization of the wavefunction cause the condensation to the ground state in the phase space (\mathbf{r}, \mathbf{p}) . The phase transition to the condensate at a certain temperature is BEC.

10B.1 Bose-Einstein condensation of ideal gas

Let us consider spin 0 ideal Bose gas. For the Bose distribution

$$f(\epsilon) = \frac{1}{e^{(\epsilon-\mu)\beta} - 1} \quad (\beta \equiv (k_B T)^{-1}) \quad (10B.4)$$

we define the point of $\mu = 0$ as follows. At $T = 0$, from (10B.4) all the particles fall into the ground state, there we define

$$\mu(T = 0) = 0. \quad (10B.5)$$

At finite temperatures, let N be the number of particles in the system:

$$N = \sum_i f(\epsilon_i).$$

^{*1} The acronym of BEC is applied to both Bose-Einstein Condensation and Bose-Einstein Condensate. In actual use, the confusion is not serious.

In the usual case we can write

$$N \rightarrow \int f(\epsilon) \mathcal{D}(\epsilon) d\epsilon. \quad (?)$$

Here the number of particle at the ground state N_0 should be

$$N_0 = \frac{1}{e^{-\mu\beta} - 1} \sim \frac{1}{-\mu\beta} = -\frac{k_B T}{\mu} \rightarrow \mu \sim -\frac{k_B T}{N_0}. \quad (10B.6)$$

If we calculate the particle distribution on this line, for three dimensional ideal gas

$$\epsilon(k) = \frac{\hbar^2 k^2}{2m} \quad \text{then} \quad \mathcal{D}(\epsilon) = \frac{m^{3/2} V}{\sqrt{2\pi^2 \hbar^3}} \sqrt{\epsilon}. \quad (10B.7)$$

Therefore

$$N = \frac{V m^{3/2}}{\sqrt{2\pi^2 \hbar^3}} \int_0^\infty \frac{\sqrt{\epsilon}}{e^{(\epsilon-\mu)\beta} - 1} d\epsilon = \frac{(m k_B T)^{3/2}}{\sqrt{2\pi^2 \hbar^3}} V \int_0^\infty \frac{\sqrt{x}}{e^{x-\alpha} - 1} dx, \quad (10B.8)$$

where $x \equiv \epsilon\beta$ and $\alpha \equiv \mu\beta$. We write the definite integral term as $I(\alpha)$, then I is

$$I(0) = \int_0^\infty \frac{\sqrt{x}}{e^x - 1} dx = \frac{\sqrt{\pi}}{2} \zeta\left(\frac{3}{2}\right) \sim 2.6, \quad (10B.9)$$

which decreases with increasing of the absolute value of $\alpha < 0$. Then, in this logic, with $T \rightarrow 0$ the maximum number of N determined from (10B.8) goes to zero. It is apparent that we have dropped something from the counting. That is, of course, the macroscopic number of particles fall into the ground state.

From Eq. (10B.8),

$$I(\alpha) = \frac{\sqrt{2\pi^2 \hbar^3}}{(m k_B T)^{3/2}} \frac{N}{V}.$$

When this exceeds (10B.9) at low temperatures the anomaly (increase in the particle number at the ground state.) occurs. This critical temperature T_c is

$$T < T_c \equiv \frac{2\pi \hbar^2}{m k_B} \left[\frac{N}{\zeta(3/2)V} \right]^{2/3}. \quad (10B.10)$$

Here $l \equiv (V/N)^{1/3}$ is the average distance between the particles and Eq. (10B.10) is interpreted as

$$l = \frac{h}{\zeta(3/2) \sqrt{2\pi m k_B T_c}} \sim \lambda(T = T_c). \quad (10B.11)$$

This confirms the statement that the BEC takes place when the average de Broglie wavelength is comparable with the average particle distance.

Below T_c , we add the number of ground state particles N_0 to Eq. (10B.8):

$$N = \frac{V m^{3/2}}{\sqrt{2\pi^2 \hbar^3}} \int_0^\infty \frac{\sqrt{\epsilon}}{e^{(\epsilon-\mu)\beta} - 1} d\epsilon + N_0. \quad (10B.12)$$

From Eq. (10B.6), N_0 becomes a macroscopic number for $T < T_c$, then $\mu = 0$. Therefore

$$N_0 = N - \frac{V m^{3/2}}{\sqrt{2\pi^2 \hbar^3}} \int_0^\infty \frac{\sqrt{\epsilon}}{e^{\epsilon\beta} - 1} d\epsilon = N \left[1 - \frac{V (m k_B T)^{3/2}}{N \sqrt{2\pi^2 \hbar^3}} I(0) \right] = N \left[1 - \left(\frac{T}{T_c} \right)^{3/2} \right]. \quad (10B.13)$$

This is just like a spontaneous magnetization rapidly grows to finite values below the critical temperature in the ferromagnetic transition.

The total energy of the system for $T < T_c$ is calculated as

$$E = \frac{V m^{3/2}}{\sqrt{2\pi^2 \hbar^3}} \int_0^\infty \frac{\epsilon^{3/2}}{e^{\beta\epsilon} - 1} d\epsilon \quad (10B.14)$$

$$\text{よって } T < T_c \text{ では } \int_0^\infty \frac{x^{3/2}}{e^x - 1} dx = \frac{3\sqrt{\pi}}{4} \zeta\left(\frac{5}{2}\right) \text{ より}$$

$$E = \frac{3}{2} \zeta\left(\frac{5}{2}\right) \left(\frac{m}{2\pi \hbar^2} \right)^{3/2} V (k_B T)^{5/2}. \quad (10B.15)$$

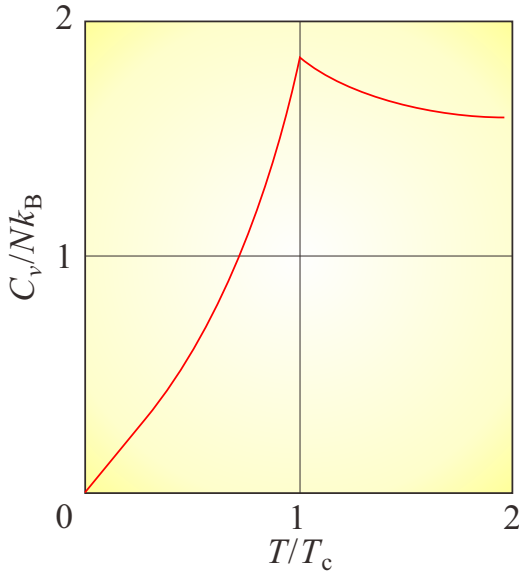


Fig. 10B.1 Specific heat at constant volume of three dimensional ideal Bose gas as a function of temperature. T_c is the critical temperature of the BEC.

Then the heat capacity at constant volume is calculated as

$$C_v = \frac{15}{4} \zeta\left(\frac{5}{2}\right) \left(\frac{m}{2\pi\hbar^2}\right)^{3/2} V k_B^{5/2} T^{3/2}. \quad (10B.16)$$

C_v shows a cusp at T_c indicating that this is the phase transition.

10B.2 Bosonic stimulation

Here we have a look at **bosonic stimulation** for N particles, which is, though, essentially the same as what has been mentioned on the case of two particles in Sed. ???. As we have seen, the bosonic stimulation works as if it is a driving force in BEC or laser oscillation. Let us consider a identical boson system the case a particle in state φ_{ini} gets perturbation and transitions to other single particel state φ_{fin} . Now the problem is the difference in the transition probabilities to the state occupied with N particles and to the empty state. We write the initial state as

$$\psi_+^{(i)}(\mathbf{r}_1, \dots, \mathbf{r}_{N+1}) = \frac{1}{\sqrt{(N+1)N! \prod_l n_l!}} \prod_{m=1}^N \hat{R}_{m,N+1} \det^{(+)}\{\varphi_i(\mathbf{r}_j)\} \varphi_{\text{ini}}(\mathbf{r}_{N+1}). \quad (10B.17)$$

The symbol $\det^{(+)}$ represents permanent, which is obtained by making the signs of all the terms into +. The final state $\psi_+^{(f)}$ is obtained by exchanging φ_{ini} with φ_{fin} . Let the matrix elements of perturbation Hamiltonian be a , i.e. $\langle \varphi_{\text{fin}} | \hat{H}_1 | \varphi_{\text{ini}} \rangle = a$.

Assuming that φ_i ($i \leq N$) is orthogonal to φ_{fin} , among $\langle \psi_+^{(f)} | \hat{H}_1 | \psi_+^{(i)} \rangle$, number of terms that give non-zero a is $(N+1)N! \prod_l n_l!$. This is equal to the sqare of the denominator in normalization constant. Then finally $\langle \psi_+^{(f)} | \hat{H}_1 | \psi_+^{(i)} \rangle = a$.

On the other hand, assuming all of φ_i ($i \leq N$) are φ_{fin} , we can write

$$\psi_+^{(i)} = \frac{1}{\sqrt{(N+1)}} \prod_{m=1}^N \hat{R}_{m,N+1} \varphi_{\text{fin}}(\mathbf{r}_1) \cdots \varphi_{\text{fin}}(\mathbf{r}_N) \varphi_{\text{ini}}(\mathbf{r}_{N+1}). \quad (10B.18)$$

All of the $N!$ terms in $\det^{(+)}$ are $\varphi_{\text{fin}}(\mathbf{r}_1) \cdots \varphi_{\text{fin}}(\mathbf{r}_N)$ and devided by $N!$ in the denominator of normalization constant to 1. However the final state is

$$\psi_+^{(f)} = \varphi_{\text{fin}}(\mathbf{r}_1) \cdots \varphi_{\text{fin}}(\mathbf{r}_N) \varphi_{\text{fin}}(\mathbf{r}_{N+1}). \quad (10B.19)$$

Then we get $\langle \varphi_{\text{fin}} | \hat{H}_1 | \varphi_{\text{ini}} \rangle = a\sqrt{N+1}$, and from the Fermi's golden rule, the transition probability should be $N+1$ times larger.

References

- [1] 高橋康. 物性研究者のための場の量子論 1 (新物理学シリーズ 16). 培風館, 10 1974.
- [2] Silvia Viola Kusminskiy. *Quantum Magnetism, Spin Waves, and Optical Cavities (SpringerBriefs in Physics)*. Springer, 2 2019.
- [3] Ryogo Kubo. The spin-wave theory of antiferromagnetics. *Phys. Rev.*, Vol. 87, pp. 568–580, Aug 1952.
- [4] Shuhei Fukuoka, Satoshi Yamashita, Yasuhiro Nakazawa, Takashi Yamamoto, Hideki Fujiwara, Takashi Shirahata, and Kazuko Takahashi. Thermodynamic properties of antiferromagnetic ordered states of $\pi - d$ interacting systems of $\kappa - (\text{BETS})_2\text{FeX}_4$ ($x = \text{Br}, \text{Cl}$). *Phys. Rev. B*, Vol. 93, p. 245136, Jun 2016.
- [5] H.B. Nielsen and S. Chadha. On how to count goldstone bosons. *Nuclear Physics B*, Vol. 105, No. 3, pp. 445–453, March 1976.
- [6] PHILIP W. ANDERSON. *BASIC NOTIONS OF CONDENSED MATTER PHYSIC*. TAYLOR & FRANCIS, 2 2019.
- [7] Haruki Watanabe and Hitoshi Murayama. Unified description of nambu-goldstone bosons without lorentz invariance. *Phys. Rev. Lett.*, Vol. 108, p. 251602, Jun 2012.
- [8] Yoshimasa Hidaka. Counting rule for nambu-goldstone modes in nonrelativistic systems. *Phys. Rev. Lett.*, Vol. 110, p. 091601, Feb 2013.
- [9] Yoshimasa Hidaka and Yuki Minami. Spontaneous symmetry breaking and nambu-goldstone modes in open classical and quantum systems. *Progress of Theoretical and Experimental Physics*, Vol. 2020, No. 3, March 2020.
- [10] H.Y. Yuan, Yunshan Cao, Akashdeep Kamra, Rembert A. Duine, and Peng Yan. Quantum magnonics: When magnon spintronics meets quantum information science. *Physics Reports*, Vol. 965, pp. 1–74, June 2022.
- [11] Philipp Pirro, Vitaliy I. Vasyuchka, Alexander A. Serga, and Burkard Hillebrands. Advances in coherent magnonics. *Nature Reviews Materials*, Vol. 6, No. 12, pp. 1114–1135, July 2021.
- [12] Sergio M. Rezende. *Fundamentals of Magnonics (Lecture Notes in Physics)*. Springer, 8 2020.
- [13] G. G. Low, A. Okazaki, R. W. H. Stevenson, and K. C. Turberfield. A measurement of spin-wave dispersion in MnF_2 at 4.2 k. *Journal of Applied Physics*, Vol. 35, No. 3, pp. 998–999, March 1964.
- [14] 高橋康. 物性研究者のための場の量子論 2 (新物理学シリーズ 17). 培風館, 4 1976.
- [15] S. O. Demokritov, V. E. Demidov, O. Dzyapko, G. A. Melkov, A. A. Serga, B. Hillebrands, and A. N. Slavin. Bose-einstein condensation of quasi-equilibrium magnons at room temperature under pumping. *Nature*, Vol. 443, No. 7110, pp. 430–433, September 2006.
- [16] T. Nikuni, M. Oshikawa, A. Oosawa, and H. Tanaka. Bose-einstein condensation of dilute magnons in tlcucl_3 . *Phys. Rev. Lett.*, Vol. 84, pp. 5868–5871, Jun 2000.
- [17] Hidekazu Tanaka, Akira Oosawa, Tetsuya Kato, Hidehiro Uekusa, Yuji Ohashi, Kazuhisa Kakurai, and Andreas Hoser. Observation of field-induced transverse néel ordering in the spin gap system TlCuCl_3 . *Journal of the Physical Society of Japan*, Vol. 70, No. 4, pp. 939–942, April 2001.
- [18] Masashi Tachiki and Takemi Yamada. Spin ordering and thermodynamical properties in spin-pair systems under magnetic fields. *Progress of Theoretical Physics Supplement*, Vol. 46, pp. 291–309, 1970.